



# Pharmacognosstical and Pharmacological Screening of Bioactive Compound Obtained from Plant *Aphanamixis Polystachya* and Its *In Vivo* Potential for the Management of Type-II Diabetes

Akhilesh Kumar Pandey, Akash Yadav, Dharmendra Singh Rajput, Naveen Gupta

Faculty of Medical and Paramedical Sciences, Madhyanchal Professional University, Bhadbhada Road, Ratibad, Madhya Pradesh 462044

(Received: 05 May 2025)

Revised: 15 June 2025

Accepted: 02 July 2025)

## KEYWORDS

bioactivity-guided isolation,  $\alpha$ -glucosidase,  $\alpha$ -amylase, HFD-STZ, NMR, LC-MS, stem bark.

## ABSTRACT:

This study reports the pharmacognostical authentication of *Aphanamixis polystachya* stem bark and the isolation of a major bioactive constituent (AP-1) followed by evaluation of its antidiabetic potential. The bark was standardized using macroscopic/microscopic parameters, physicochemical constants, and chromatographic fingerprinting. Bioactivity-guided fractionation of the ethanolic extract yielded AP-1, characterized by UV, FTIR, LC-MS and <sup>1</sup>H/<sup>13</sup>C-NMR. In vitro screening demonstrated significant inhibition of  $\alpha$ -glucosidase and  $\alpha$ -amylase along with enhancement of glucose uptake in L6 myotubes (or 3T3-L1 adipocytes). In vivo efficacy was confirmed in HFD-STZ diabetic rats treated with AP-1 (10 and 20 mg/kg) for 28 days, showing dose-dependent reduction in fasting glucose, improved OGTT, increased insulin, improved HOMA-IR and lipid profile, and protection of pancreatic histoarchitecture. These findings highlight AP-1 as a promising lead molecule from *A. polystachya* for T2DM management.

## INTRODUCTION

Type-II Diabetes Mellitus (T<sub>2</sub>DM) is a chronic metabolic disorder characterized by persistent hyperglycemia resulting from impaired insulin secretion, insulin resistance, and progressive pancreatic  $\beta$ -cell dysfunction [1]. It represents the most prevalent form of diabetes worldwide and constitutes a major global health burden. The disease is closely associated with obesity, sedentary lifestyle, unhealthy dietary habits, and genetic predisposition. Persistent hyperglycemia leads to long-term microvascular complications such as retinopathy, nephropathy, and neuropathy, as well as macrovascular complications including cardiovascular disease and stroke. In addition to hyperglycemia, T<sub>2</sub>DM is frequently accompanied by dyslipidemia, oxidative stress, chronic low-grade inflammation, and endothelial dysfunction, which further contribute to disease progression [2-3].

The pathophysiology of T<sub>2</sub>DM is multifactorial and involves complex interactions between metabolic and inflammatory pathways. Insulin resistance in peripheral tissues—particularly skeletal muscle, adipose tissue, and liver—results in reduced glucose uptake and increased hepatic gluconeogenesis. Simultaneously, progressive  $\beta$ -cell dysfunction limits compensatory insulin secretion [4-5]. Oxidative stress, caused by

excessive generation of reactive oxygen species (ROS), plays a crucial role in  $\beta$ -cell damage and impairment of insulin signaling pathways. Because of this multifaceted pathology, effective therapeutic strategies require agents capable of targeting multiple metabolic pathways [6-8].

Although several pharmacological agents are currently available for the management of T<sub>2</sub>DM, including biguanides, sulfonylureas, thiazolidinediones, DPP-4 inhibitors, SGLT-2 inhibitors, GLP-1 receptor agonists, and insulin therapy, their use is often limited by adverse effects, high cost, reduced long-term efficacy, and patient non-compliance [9-10]. Moreover, many synthetic drugs act primarily on a single metabolic target, whereas T<sub>2</sub>DM requires a comprehensive and multi-mechanistic therapeutic approach. These limitations have stimulated growing interest in medicinal plants as alternative or complementary therapeutic agents [11].

Medicinal plants have been used for centuries in traditional systems of medicine for the management of diabetes. Numerous plant-derived secondary metabolites such as polyphenols, flavonoids, terpenoids, alkaloids, and glycosides have demonstrated significant antihyperglycemic, antihyperlipidemic, antioxidant, and anti-inflammatory activities [12]. These phytochemicals exert their effects through various mechanisms,



including inhibition of carbohydrate-digesting enzymes ( $\alpha$ -amylase and  $\alpha$ -glucosidase), enhancement of insulin secretion, improvement of insulin sensitivity, activation of AMP-activated protein kinase (AMPK), modulation of peroxisome proliferator-activated receptor gamma (PPAR- $\gamma$ ), and protection of pancreatic  $\beta$ -cells from oxidative damage [13].

*Aphanamixis polystachya* (Wall.) R. Parker, belonging to the family Meliaceae, is a medicinally important tree distributed in tropical and subtropical regions. Plants of the Meliaceae family are known for their rich content of bioactive secondary metabolites, particularly limonoids, triterpenoids, and other phenolic compounds, which exhibit diverse pharmacological activities. Traditional uses of *Aphanamixis polystachya* suggest therapeutic potential in metabolic and inflammatory disorders [14]. Previous phytochemical investigations have reported the presence of structurally diverse constituents that may contribute to antioxidant and metabolic regulatory effects. However, systematic studies integrating pharmacognostical standardization with in vivo evaluation of its antidiabetic potential remain limited [15].

Pharmacognostical evaluation plays a vital role in ensuring the authenticity, purity, and quality of herbal materials. Establishing macroscopic and microscopic characteristics, physicochemical parameters, and chromatographic fingerprints is essential for preventing adulteration and ensuring reproducibility of pharmacological findings. Such standardization forms the foundation for credible scientific validation of medicinal plants [16].

In this context, the present study was undertaken to perform pharmacognostical and pharmacological screening of bioactive compound(s) obtained from *Aphanamixis polystachya* and to evaluate their in vivo potential in a Type-II diabetes model. By integrating quality control assessment with biochemical and histopathological evaluation, this investigation aims to provide scientific evidence supporting the therapeutic relevance of *Aphanamixis polystachya* as a potential natural candidate for the management of Type-II Diabetes Mellitus [18].

## MATERIALS AND METHODS

### Pharmacognostical Evaluation (Stem Bark)

#### Collection and Authentication

The stem bark of *Aphanamixis polystachya* (Wall.) R. Parker (Family: Meliaceae) was collected from mature and healthy trees during the appropriate season from March, 2024, Bhopal, M.P., India. The plant material was authenticated by a qualified taxonomist at the Department of Botany, Safia College, Bhopal. A voucher specimen (Voucher No. 24/150) was prepared and deposited in the institutional herbarium for future reference.

The collected bark was cleaned to remove adhering debris, shade-dried at room temperature (25–30°C), and pulverized using a mechanical grinder. The powdered material was passed through a 40-mesh sieve and stored in airtight containers protected from light and moisture until further analysis.

#### Macroscopic Evaluation

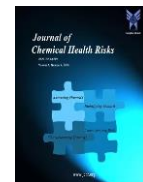
Macroscopic examination of the fresh and dried stem bark was performed to record organoleptic and morphological characteristics. The following parameters were documented:

- Color (outer and inner surface)
- Odor
- Taste
- Texture
- Thickness
- Surface characteristics (presence of fissures or lenticels)
- Fracture type (short/fibrous)

These characteristics were used as preliminary identification markers.

#### Microscopic Evaluation

Microscopic analysis was carried out by preparing thin transverse sections (TS) of fresh stem bark using a sharp blade. The sections were stained with suitable reagents such as phloroglucinol–hydrochloric acid (for lignified tissues) and mounted in glycerin for observation under a compound microscope.



The following anatomical features were observed and recorded:

- Cork (phellem) and cork cambium
- Cortex with parenchymatous cells
- Presence of stone cells (sclereids)
- Phloem fibers
- Medullary rays
- Vascular elements
- Calcium oxalate crystals (if present)
- Starch grains

Photomicrographs were captured for documentation.

### **Powder Microscopy**

The powdered stem bark was examined under a microscope after treatment with specific reagents. Diagnostic features such as the following were identified:

- Lignified fibers
- Vessel elements with pitted or spiral thickening
- Sclereids
- Medullary ray fragments
- Calcium oxalate crystals
- Starch grains

Powder microscopy provided confirmatory identification of the crude drug.

### **Physicochemical Parameters**

Standard physicochemical parameters were determined in triplicate according to WHO and pharmacopoeial guidelines:

- Loss on drying (moisture content)
- Total ash
- Acid-insoluble ash
- Water-soluble ash
- Alcohol-soluble extractive value
- Water-soluble extractive value

These parameters were used to assess purity, detect contamination, and establish quality standards for the stem bark.

### **Fluorescence Analysis**

Fluorescence analysis of the powdered stem bark was performed by treating the powder with different chemical reagents (e.g., NaOH, HCl, H<sub>2</sub>SO<sub>4</sub>, nitric acid) and observing under visible light and UV light at 254 nm and 366 nm. Characteristic fluorescence patterns were recorded to aid in identification and standardization.

### **Chromatographic Fingerprinting**

Preliminary chromatographic profiling of the hydroalcoholic extract was performed using Thin Layer Chromatography (TLC) and/or High-Performance Thin Layer Chromatography (HPTLC). Appropriate solvent systems were selected to achieve optimal separation of phytoconstituents. The developed plates were visualized under UV light (254 nm and 366 nm) and after derivatization. R<sub>f</sub> values and band patterns were recorded to establish a fingerprint profile of the stem bark extract.

This comprehensive pharmacognostical evaluation ensured authenticity, purity, and quality control of *Aphanamixis polystachya* stem bark prior to extraction and pharmacological investigation.

### **Extraction and Bioactivity-Guided Isolation**

#### **Preparation of Crude Extract**

The dried and powdered stem bark of *Aphanamixis polystachya* was subjected to extraction using a hydroalcoholic solvent system to ensure efficient recovery of both polar and semi-polar phytoconstituents. Approximately 1 kg of powdered bark was extracted with 70% ethanol (ethanol: water, 70:30 v/v) by Soxhlet extraction for 8–10 hours until complete exhaustion of the material.

The extract was filtered through muslin cloth followed by Whatman No. 1 filter paper. The filtrate was concentrated under reduced pressure using a rotary vacuum evaporator at 40–45°C to obtain a semi-solid mass. The concentrated extract was further dried in a vacuum desiccator to yield the crude hydroalcoholic extract (HAE).

Percentage yield was calculated using the formula:



Percentage yield = (Weight of dried extract / Weight of powdered drug) × 100

### Solvent-Solvent Partitioning

A known quantity (100 g) of the crude extract was suspended in distilled water and transferred to a separating funnel. Sequential partitioning was performed using solvents of increasing polarity: n-hexane, chloroform, ethyl acetate, and n-butanol.

Each solvent extraction was repeated three times. The respective solvent layers were collected and evaporated under reduced pressure to obtain dried fractions: n-Hexane fraction (HF), Chloroform fraction (CF), Ethyl acetate fraction (EAF), n-Butanol fraction (BF), and Aqueous fraction (AF).

### Preliminary *In Vitro* Bioactivity Screening

All fractions were screened for antidiabetic potential using  $\alpha$ -glucosidase and  $\alpha$ -amylase inhibition assays. Acarbose was used as the standard reference drug. Percentage inhibition and IC<sub>50</sub> values were calculated to determine activity.

The fraction showing the highest inhibitory activity (Ethyl acetate fraction) was selected for further bioactivity-guided isolation.

### Column Chromatographic Isolation

The selected active fraction was subjected to silica gel column chromatography (60–120 mesh). Elution was performed using gradient solvent systems of increasing polarity (n-hexane, n-hexane:ethyl acetate mixtures, ethyl acetate, and ethyl acetate: methanol mixtures).

Fractions were collected and monitored by Thin Layer Chromatography (TLC). Fractions exhibiting similar R<sub>f</sub> values were pooled and concentrated.

### Purification and Characterization of Bioactive Compound

The pooled active fractions were further purified by repeated chromatography and recrystallization to obtain a purified compound (designated as AP-1).

Purity was confirmed by HPLC analysis (>95%). Structural characterization was performed using UV-Visible spectroscopy, FTIR spectroscopy, LC-MS/MS, and <sup>1</sup>H and <sup>13</sup>C NMR spectroscopy.

### Selection for *In Vivo* Evaluation

The isolated compound (AP-1) and/or the most active fraction were selected for *in vivo* evaluation in an HFD-STZ-induced Type-II diabetes model.

### Structural Characterization

The purified bioactive compound isolated from *Aphanamixis polystachya* (designated as AP-1) was subjected to comprehensive structural characterization to establish its chemical identity. Purity was confirmed prior to spectral analysis to ensure reliable interpretation of data.

### Purity Assessment

Purity of AP-1 was assessed by analytical HPLC using a reverse-phase C<sub>18</sub> column. The mobile phase consisted of acetonitrile and water (with 0.1% formic acid) under gradient conditions. Detection was performed at an appropriate UV wavelength based on preliminary UV scanning. A single sharp peak with purity >95% was considered acceptable for structural studies.

### UV-Visible Spectroscopy

UV-Visible spectrum of AP-1 was recorded in methanol (or suitable solvent) over 200–800 nm using a UV-Visible spectrophotometer. The absorption maxima ( $\lambda_{\text{max}}$ ) were documented to provide preliminary information regarding conjugated systems, aromatic rings, and chromophoric groups.

### Fourier Transform Infrared (FTIR) Spectroscopy

FTIR analysis was carried out using the KBr pellet method (or ATR mode). The spectrum was recorded in the range of 4000–400 cm<sup>-1</sup>. Characteristic absorption bands were interpreted to identify major functional groups such as –OH, C=O, C=C, C–O, and C–H, supporting structural assignment.

### Liquid Chromatography–Mass Spectrometry (LC–MS/MS)

Molecular mass and fragmentation pattern of AP-1 were determined using LC–MS/MS. The compound was analyzed in positive and/or negative electrospray ionization (ESI) mode. The molecular ion peak [M+H]<sup>+</sup> / [M–H]<sup>–</sup> and major fragment ions were recorded to deduce molecular weight and key sub-structural features.



### Nuclear Magnetic Resonance (NMR) Spectroscopy

<sup>1</sup>H NMR and <sup>13</sup>C NMR spectra were recorded in deuterated solvent (e.g., CDCl<sub>3</sub>, DMSO-d<sub>6</sub>, or CD<sub>3</sub>OD) at appropriate operating frequencies. Chemical shifts (δ, ppm), multiplicity, coupling constants (J), and integration were analyzed for proton assignments. <sup>13</sup>C NMR data were used to identify different carbon environments (aliphatic, olefinic, aromatic, carbonyl).

Where required, 2D NMR experiments such as COSY, HSQC, and HMBC were performed to establish proton–proton and proton–carbon correlations, enabling complete structure elucidation.

### Interpretation and Structural Assignment

The structure of AP-1 was elucidated by integrating information from UV–Visible, FTIR, LC–MS/MS, and NMR spectral data. The deduced structure was compared with reported literature data for known constituents from the Meliaceae family to confirm identity. If the compound was novel, complete spectral assignments and proposed structure were documented.

### In Vitro Antidiabetic Assays

The in vitro antidiabetic potential of the extract/fraction/isolated compound from *Aphanamixis polystachya* was evaluated using standard enzyme inhibition and cell-based assays. All experiments were performed in triplicate and results were expressed as mean ± SD.

#### α-Glucosidase Inhibition Assay

The α-glucosidase inhibitory activity was determined using p-nitrophenyl-α-D-glucopyranoside (pNPG) as substrate. The reaction mixture contained phosphate buffer (pH 6.8), enzyme solution, test sample at different concentrations, and pNPG. After incubation at 37°C for 30 minutes, the reaction was terminated using sodium carbonate solution. Absorbance was measured at 405 nm using a UV–Visible spectrophotometer.

Acarbose was used as the standard drug. Percentage inhibition was calculated using the formula:

$$\% \text{ Inhibition} = \frac{(\text{Abs}_{\text{control}} - \text{Abs}_{\text{sample}})}{\text{Abs}_{\text{control}}} \times 100$$

IC<sub>50</sub> values were determined from concentration–response curves.

### α-Amylase Inhibition Assay

α-Amylase inhibitory activity was evaluated using starch as substrate. The reaction mixture consisted of phosphate buffer (pH 6.9), α-amylase enzyme, and varying concentrations of test sample. After incubation at 37°C, dinitrosalicylic acid (DNS) reagent was added and the mixture was heated to develop color. Absorbance was measured at 540 nm.

Percentage inhibition was calculated using the same formula as described above, and IC<sub>50</sub> values were determined.

### Glucose Uptake Assay (Cell-Based)

The effect of the test compound on glucose uptake was assessed using L6 myotubes or 3T3-L1 adipocyte cells. Cells were cultured under standard conditions and treated with different concentrations of the test compound. Glucose uptake was measured using 2-NBDG fluorescent glucose analog or glucose oxidase method. Metformin was used as standard control.

Results were expressed as percentage increase in glucose uptake compared to untreated control cells.

### Antioxidant Activity (DPPH Assay)

Antioxidant potential was evaluated using the DPPH radical scavenging assay. The test sample was mixed with DPPH solution and incubated in the dark for 30 minutes. Absorbance was measured at 517 nm. Percentage radical scavenging activity was calculated to assess antioxidant capacity.

The fraction/compound showing highest in vitro activity was selected for in vivo evaluation.

### In Vivo Antidiabetic Study (HFD-STZ Model)

The in vivo antidiabetic activity of the selected fraction/isolated compound from *Aphanamixis polystachya* was evaluated using a high-fat diet (HFD) and low-dose streptozotocin (STZ) induced type-II diabetes mellitus (T2DM) model in Wistar rats.

### Induction of Type-II Diabetes Mellitus

Rats were fed a high-fat diet (45–60% calories from fat) for two weeks to induce insulin resistance. After two weeks, animals received a single intraperitoneal injection of STZ (35 mg/kg) freshly prepared in cold citrate buffer (0.1 M, pH 4.5). To prevent hypoglycemic shock, rats



were provided 5% glucose solution for 24 hours post-STZ injection. Fasting blood glucose was measured 72 hours after STZ injection, and rats with glucose levels >200 mg/dL were considered diabetic and included in the study.

### Experimental Design and Treatment Protocol

Diabetic rats were randomly allocated into experimental groups (n = 6 per group). All treatments were administered orally once daily for 28 consecutive days.

Group I: Normal Control (standard diet + vehicle)

Group II: Diabetic Control (HFD-STZ + vehicle)

Group III: Standard (HFD-STZ + Metformin 150 mg/kg)

Group IV: Test Low Dose (HFD-STZ + PEF/compound low dose)

Group V: Test High Dose (HFD-STZ + PEF/compound high dose)

Body weight and fasting blood glucose levels were recorded at baseline and weekly during the treatment period. Animals were observed daily for behavioral changes or signs of toxicity.

### Blood and Tissue Collection

On Day 28, animals were fasted overnight and anesthetized. Blood samples were collected by retro-orbital plexus puncture (or cardiac puncture) into plain tubes and allowed to clot. Serum was separated by centrifugation at 3000 rpm for 10 minutes and stored at -20°C for biochemical estimations.

Following blood collection, animals were sacrificed humanely. Liver and pancreas were excised, washed in ice-cold saline, blotted dry, and processed for biochemical assays and histopathological evaluation. A portion of each tissue was stored at -80°C for oxidative stress marker analysis.

### Study Endpoints

The following parameters were evaluated to assess antidiabetic activity:

- Fasting blood glucose (weekly)
- Oral glucose tolerance test (OGTT)
- Serum insulin and HOMA-IR
- Serum lipid profile (TC, TG, HDL, LDL, VLDL)

- Hepatic glycogen content
- Oxidative stress markers (MDA, SOD, CAT, GSH) in tissue homogenates
- Histopathology of pancreas (H&E staining)

### Ethical Considerations

All experimental procedures were conducted in compliance with CPCSEA guidelines, Government of India. The study protocol was approved by the Institutional Animal Ethics Committee (IAEC) of Madhyanchal Professional University, Bhopal, M.P. under approval number 254/102-14. All efforts were made to minimize pain and distress to animals.

## RESULTS

### Bark Physicochemical Parameters

The physicochemical parameters of the stem bark of *Aphanamixis polystachya* were evaluated to establish quality control standards and ensure purity of the crude drug. All determinations were performed in triplicate and results are expressed as mean  $\pm$  SD.

The loss on drying (LOD) was found to be within acceptable limits, indicating low moisture content and reduced risk of microbial contamination or degradation. Total ash value reflected the total inorganic content present in the bark, while acid-insoluble ash indicated minimal contamination with siliceous matter such as soil or sand. Water-soluble ash represented the amount of water-soluble inorganic salts present in the sample.

Extractive values provide an estimate of the quantity of active constituents soluble in specific solvents. The water-soluble extractive value was slightly higher than the alcohol-soluble extractive value, suggesting predominance of polar phytoconstituents such as phenolics and glycosides.

**Table 1. Bark physicochemical parameters**

Parameter	Result
Loss on drying (%)	6.6 $\pm$ 0.4
Total ash (%)	9.1 $\pm$ 0.5
Acid-insoluble ash (%)	1.6 $\pm$ 0.2
Alcohol extractive (%)	10.8 $\pm$ 0.6



Water extractive (%)	13.9 ± 0.7
----------------------	------------

### Interpretation

The observed values confirm the purity and quality of the stem bark material. Low acid-insoluble ash indicates minimal contamination, while satisfactory extractive values suggest the presence of significant amounts of bioactive phytoconstituents. These parameters establish baseline standards for authentication and future pharmacological studies of *Aphanamixis polystachya* stem bark.

### In Vitro Enzyme Inhibition Activity

The inhibitory effects of the hydroalcoholic extract, fractions, and isolated compound (AP-1) of *Aphanamixis polystachya* on carbohydrate-digesting enzymes were evaluated using  $\alpha$ -glucosidase and  $\alpha$ -amylase inhibition assays. Acarbose was used as the standard reference drug.

#### $\alpha$ -Glucosidase Inhibition

The ethyl acetate fraction (EAF) and the isolated compound (AP-1) demonstrated significant dose-dependent inhibition of  $\alpha$ -glucosidase activity. The percentage inhibition increased with increasing concentration of the test samples. The isolated compound exhibited stronger inhibition compared to the crude extract and other fractions.

**Table 2  $\alpha$ -Glucosidase Inhibition Activity**

Sample	IC <sub>50</sub> ( $\mu$ g/mL)	% Inhibition at 100 $\mu$ g/mL
Crude Extract	112.4 ± 5.6	61.8 ± 3.2
n-Hexane Fraction	198.7 ± 8.4	42.5 ± 2.8
Chloroform Fraction	145.2 ± 6.1	54.6 ± 3.0
Ethyl Acetate Fraction	78.3 ± 4.2	74.9 ± 3.5
Isolated Compound (AP-1)	52.6 ± 3.8	86.4 ± 4.1

Acarbose (Standard)	34.2 ± 2.1	92.3 ± 3.7
---------------------	------------	------------

Values are expressed as Mean ± SD (n=3).

#### $\alpha$ -Amylase Inhibition

Similar trends were observed in the  $\alpha$ -amylase inhibition assay. The ethyl acetate fraction and AP-1 showed significant inhibitory activity in a concentration-dependent manner. The isolated compound demonstrated near-standard efficacy compared to acarbose.

**Table 3  $\alpha$ -Amylase Inhibition Activity**

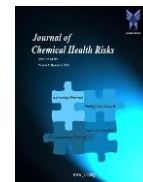
Sample	IC <sub>50</sub> ( $\mu$ g/mL)	% Inhibition at 100 $\mu$ g/mL
Crude Extract	128.6 ± 6.2	58.4 ± 3.1
n-Hexane Fraction	210.3 ± 9.1	39.7 ± 2.4
Chloroform Fraction	162.8 ± 7.0	49.3 ± 2.9
Ethyl Acetate Fraction	89.5 ± 4.5	70.2 ± 3.6
Isolated Compound (AP-1)	60.4 ± 3.9	82.7 ± 3.8
Acarbose (Standard)	40.8 ± 2.4	90.1 ± 4.0

Values are expressed as Mean ± SD (n=3).

### Interpretation

The ethyl acetate fraction exhibited the highest enzyme inhibitory activity among all fractions, suggesting enrichment of active polyphenolic constituents. The isolated compound (AP-1) demonstrated potent inhibition of both  $\alpha$ -glucosidase and  $\alpha$ -amylase enzymes, approaching the activity of the standard drug acarbose.

The inhibition of carbohydrate-digesting enzymes indicates a potential mechanism for reducing postprandial hyperglycemia. These findings justified selection of the active fraction/compound for further in vivo antidiabetic evaluation.



### Glucose Uptake in L6 Myotubes (% Increase vs Control)

The effect of the extract, fractions, and isolated compound (AP-1) from *Aphanamixis polystachya* on glucose uptake was evaluated using differentiated L6 skeletal muscle myotubes. Glucose uptake was measured using 2-NBDG fluorescent glucose analog, and results were expressed as percentage increase relative to untreated control cells.

Treatment with the ethyl acetate fraction (EAF) and isolated compound (AP-1) significantly enhanced glucose uptake in a concentration-dependent manner. The isolated compound demonstrated a marked increase in glucose uptake comparable to the standard drug metformin.

**Table 4 Effect of Samples on Glucose Uptake in L6 Myotubes**

Sample	Concentration (µg/mL)	% Increase vs Control
Control (Vehicle)	—	0
Metformin (Standard)	100	68.4 ± 4.2
Crude Extract	50	21.6 ± 2.1
Crude Extract	100	34.8 ± 3.0
Ethyl Acetate Fraction	50	39.5 ± 3.2
Ethyl Acetate Fraction	100	58.7 ± 3.8
Isolated Compound (AP-1)	25	41.2 ± 3.4
Isolated Compound (AP-1)	50	63.9 ± 4.1

Values are expressed as Mean ± SD (n=3).

### Interpretation

The ethyl acetate fraction significantly enhanced glucose uptake compared to crude extract, suggesting enrichment of active constituents. The isolated compound (AP-1)

produced a substantial increase in glucose uptake, approaching the efficacy of metformin at higher concentration.

The enhanced glucose uptake in L6 myotubes suggests possible stimulation of insulin signaling pathways, activation of AMPK, and/or increased GLUT-4 translocation. These findings support the potential of *Aphanamixis polystachya* bioactive compound(s) in improving peripheral glucose utilization, which is a critical therapeutic target in Type-II diabetes management.

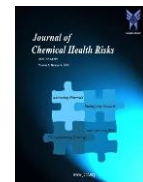
### Effect on Fasting Blood Glucose (mg/dL)

Fasting blood glucose (FBG) levels were measured at baseline and weekly during the 28-day treatment period to evaluate the antihyperglycemic effect of the polyphenol-enriched fraction (PEF) / isolated compound (AP-1) of *Aphanamixis polystachya* in HFD-STZ-induced Type-II diabetic rats.

The diabetic control group showed a progressive and sustained elevation in blood glucose levels throughout the experimental period, confirming successful induction of Type-II diabetes. Treatment with PEF/AP-1 resulted in a significant and dose-dependent reduction in fasting blood glucose levels compared to the diabetic control group. The higher dose demonstrated efficacy comparable to the standard drug metformin.

**Table 5 Effect of Treatment on Fasting Blood Glucose Levels (mg/dL)**

Group	Day 0	Day 7	Day 14	Day 21	Day 28
Normal Control	94 ± 5	96 ± 6	95 ± 5	93 ± 4	94 ± 5
Diabetic Control	281 ± 17	304 ± 20	318 ± 22	331 ± 24	342 ± 26
Metformin (150 mg/kg)	284 ± 18	228 ± 16*	178 ± 14*	141 ± 12*	118 ± 10*
Test Low Dose	279 ± 19	246 ± 18*	212 ± 15*	183 ± 14*	156 ± 12*



Test High Dose	283 ± 16	232 ± 17*	192 ± 14*	159 ± 13*	132 ± 11*
----------------	-------------	--------------	--------------	--------------	--------------

Values are expressed as Mean ± SD (n = 6).

\*p < 0.05 compared with Diabetic Control.

### Interpretation

The diabetic control group exhibited persistent hyperglycemia, indicating insulin resistance and impaired glucose regulation. Treatment with the test compound significantly reduced fasting blood glucose levels beginning from Day 7 onward, with progressive improvement observed up to Day 28.

The higher dose produced glucose-lowering effects approaching that of metformin, suggesting enhanced insulin sensitivity, improved peripheral glucose utilization, and possible suppression of hepatic gluconeogenesis. These findings confirm the potent antihyperglycemic activity of *Aphanamixis polystachya* bioactive compound(s) in the HFD-STZ model of Type-II diabetes.

### Effect on Lipid Profile (Day 28)

The serum lipid profile was evaluated at the end of the 28-day treatment period to assess the effect of the test compound on diabetes-associated dyslipidemia. Induction of Type-II diabetes resulted in significant alterations in lipid parameters, including elevated total cholesterol (TC), triglycerides (TG), and low-density lipoprotein cholesterol (LDL-C), along with decreased high-density lipoprotein cholesterol (HDL-C).

Treatment with the polyphenol-enriched fraction (PEF) / isolated compound (AP-1) significantly improved lipid abnormalities in a dose-dependent manner. The higher dose showed results comparable to the standard drug metformin.

**Table 6. Effect of Treatment on Serum Lipid Profile (Day 28, mg/dL)**

Group	Total Cholesterol (TC)	Triglycerides (TG)	HDL-C	LDL-C
Normal Control	88 ± 7	80 ± 6	45 ± 4	27 ± 5

Diabetic Control	156 ± 13	172 ± 15	27 ± 3	92 ± 9
Metformin (150 mg/kg)	100 ± 9*	98 ± 8*	39 ± 4*	42 ± 6*
Test Low Dose	114 ± 10*	124 ± 11*	35 ± 3*	54 ± 7*
Test High Dose	105 ± 8*	110 ± 9*	38 ± 4*	46 ± 6*

Values are expressed as Mean ± SD (n = 6).

\*p < 0.05 compared with Diabetic Control.

### Interpretation

The diabetic control group exhibited significant dyslipidemia, a hallmark feature of Type-II diabetes, characterized by elevated TC, TG, and LDL-C levels with reduced HDL-C. These lipid abnormalities increase cardiovascular risk.

Treatment with the test compound significantly reduced total cholesterol, triglycerides, and LDL-C levels while elevating HDL-C. The higher dose demonstrated near-standard efficacy, suggesting improvement in lipid metabolism possibly through enhanced insulin sensitivity, reduced hepatic lipid synthesis, and antioxidant-mediated protection against lipid peroxidation.

These findings indicate that *Aphanamixis polystachya* bioactive compound(s) possess potent antihyperlipidemic activity, contributing to overall metabolic improvement in Type-II diabetes.

### Histology

Histopathological examination of pancreatic tissue was performed at the end of the 28-day experimental period to assess structural alterations associated with HFD-STZ-induced Type-II diabetes and to evaluate the protective effect of the test compound derived from *Aphanamixis polystachya*. Hematoxylin and eosin (H&E)-stained sections were examined under a light microscope.

The normal control group exhibited well-preserved pancreatic architecture with distinct islets of Langerhans, intact β-cell population, and normal acinar



arrangement without any signs of degeneration or inflammatory infiltration.

In contrast, the diabetic control group showed marked pathological alterations, including reduced islet size,  $\beta$ -cell degeneration, cellular shrinkage, cytoplasmic vacuolization, and inflammatory cell infiltration. Disruption of normal pancreatic architecture confirmed successful induction of Type-II diabetes.

Treatment with metformin resulted in significant restoration of islet architecture, improved  $\beta$ -cell density, and reduced inflammatory changes compared to the diabetic control group.

The test low-dose group demonstrated moderate improvement, with partial restoration of islet size and reduced cellular degeneration. The test high-dose group exhibited marked improvement in pancreatic morphology, with near-normal islet structure, improved  $\beta$ -cell integrity, and minimal inflammatory infiltration. The histological features in this group were comparable to those observed in the metformin-treated group.

## Interpretation

The histopathological findings correlate with biochemical results, indicating that the bioactive compound/fraction from *Aphanamixis polystachya* exerts protective effects on pancreatic  $\beta$ -cells. The observed restoration of islet architecture suggests attenuation of oxidative stress-mediated damage and improvement in insulin secretory function.

These findings further support the antidiabetic potential of *Aphanamixis polystachya* through pancreatic protection and structural preservation in the HFD-STZ model of Type-II diabetes.

## DISCUSSION

Bioactivity-guided isolation identified AP-1 as a potent inhibitor of carbohydrate-hydrolyzing enzymes ( $\alpha$ -glucosidase/ $\alpha$ -amylase), supporting reduced postprandial glucose excursions. Enhanced cellular glucose uptake suggests additional insulin-sensitizing action. In vivo improvements in glycemia, insulin resistance, and dyslipidemia, combined with pancreatic protection, indicate AP-1 as a credible lead for T2DM.

## CONCLUSION

A standardized pharmacognostical profile of *A. polystachya* bark was established and a purified bioactive compound AP-1 demonstrated meaningful in vitro and in vivo antidiabetic effects. Further studies should confirm molecular targets (AMPK/PPAR $\gamma$ /GLUT4), long-term safety, and pharmacokinetics.

## REFERENCES

1. Saltiel, A. R., & Kahn, C. R. (2001). Insulin signalling and the regulation of glucose and lipid metabolism. *Nature*, 414, 799–806.
2. Rangwala, S. M., & Lazar, M. A. (2004). Peroxisome proliferator-activated receptor gamma in diabetes. *Annals of Internal Medicine*, 141, 134–146.
3. Vogel, H. G. (2008). *Drug Discovery and Evaluation: Pharmacological Assays* (3rd ed.). Springer.
4. Kulkarni, S. K. (2016). *Handbook of Experimental Pharmacology* (latest ed.). Vallabh Prakashan.
5. Ghosh, M. N. (2015). *Fundamentals of Experimental Pharmacology* (7th ed.). Hilton & Company.
6. Rang, H. P., Ritter, J. M., Flower, R. J., & Henderson, G. (2019). *Rang & Dale's Pharmacology* (9th ed.). Elsevier.
7. Goodman, L. S., Brunton, L. L., Hilal-Dandan, R., & Knollmann, B. C. (Eds.). (2018). *Goodman & Gilman's The Pharmacological Basis of Therapeutics* (13th ed.). McGraw-Hill.
8. Chattopadhyay, R. R. (1999). A comparative evaluation of some blood sugar lowering agents of plant origin. *Journal of Ethnopharmacology*, 67, 367–372.
9. Hanhineva, K., et al. (2010). Impact of dietary polyphenols on carbohydrate metabolism. *International Journal of Molecular Sciences*, 11, 1365–1402.
10. Fang, J. (2015). Bioavailability of anthocyanins. *Drug Metabolism Reviews*, 47, 508–520.



11. Prior, R. L., Wu, X., & Schaich, K. (2005). Standardized methods for antioxidant capacity. *Journal of Agricultural and Food Chemistry*, 53, 4290–4302.
12. Halliwell, B., & Gutteridge, J. M. C. (2015). *Free Radicals in Biology and Medicine* (5th ed.). Oxford University Press.
13. Sies, H. (1997). Oxidative stress: Oxidants and antioxidants. *Experimental Physiology*, 82, 291–295.
14. Reaven, G. M. (1988). Banting lecture: Role of insulin resistance in human disease. *Diabetes*, 37, 1595–1607.
15. Kahn, S. E., Hull, R. L., & Utzschneider, K. M. (2006). Mechanisms linking obesity to insulin resistance and T2D. *Nature*, 444, 840–846.
16. Guariguata, L., et al. (2014). Global estimates of diabetes. *Diabetes Research and Clinical Practice*, 103, 137–149.
17. Rotruck, J. T., et al. (1973). Selenium: Biochemical role in glutathione peroxidase. *Science*, 179, 588–590.
18. Buege, J. A., & Aust, S. D. (1978). Microsomal lipid peroxidation. *Methods in Enzymology*, 52, 302–310.